



OPEN ACCESS

EDITED BY

Kunimasa Ohta,
Kyushu University, Japan

REVIEWED BY

Yasuko Akiyama-Oda,
JT Biohistory Research Hall, Japan
Yuki Maeda,
RIKEN Center for Brain Science (CBS), Japan

*CORRESPONDENCE

Yoshiko Takahashi,
✉ yotayota@develop.zool.kyoto-u.ac.jp
Masafumi Inaba,
✉ inaba.masafumi.5r@kyoto-u.ac.jp

RECEIVED 18 November 2024

ACCEPTED 07 February 2025

PUBLISHED 27 February 2025

CITATION

Kawamura K, Kato S, Utsunomiya S, Takahashi Y
and Inaba M (2025) Self-organized patterning of
peristaltic waves by suppressive actions in a
developing gut.
Front. Cell Dev. Biol. 13:1529975.
doi: 10.3389/fcell.2025.1529975

COPYRIGHT

© 2025 Kawamura, Kato, Utsunomiya,
Takahashi and Inaba. This is an open-access
article distributed under the terms of the
[Creative Commons Attribution License \(CC BY\)](https://creativecommons.org/licenses/by/4.0/).
The use, distribution or reproduction in other
forums is permitted, provided the original
author(s) and the copyright owner(s) are
credited and that the original publication in this
journal is cited, in accordance with accepted
academic practice. No use, distribution or
reproduction is permitted which does not
comply with these terms.

Self-organized patterning of peristaltic waves by suppressive actions in a developing gut

Koji Kawamura¹, Soichiro Kato², Shota Utsunomiya¹,
Yoshiko Takahashi^{1*} and Masafumi Inaba^{1*}

¹Department of Zoology, Graduate School of Science, Kyoto University, Kyoto, Japan, ²Department of Biological Sciences, Graduate School of Science, Osaka University, Toyonaka, Osaka, Japan

Gut peristalsis is a wave-like movement of a local contraction along the gut, and plays important roles in nutrient digestion and absorption. When peristaltic waves emerge in embryonic guts, randomly distributed origins of peristaltic waves (OPWs) become progressively confined to specific sites. We have investigated how this random-to-organized positioning is achieved using the caecum as a model in chicken embryos. While prominent OPWs, recognized as active (spontaneous) contractions, are located at endpoints of the intact caecum, other regions are also found to possess latent rhythm unveiled by fragmentation of a caecum into pieces, showing that the latent rhythm is normally suppressed in the intact gut. Analyses with caecum fragments demonstrate that the latent rhythm is spatially patterned in an early gut, to which negative impact by primitive passing waves contributes; the more passing waves a region experiences to undergo forced/passive contractions, the slower latent rhythm this region acquires. This patterned latent rhythm underlies the final positioning of OPWs at later stages, where a site with faster latent rhythm dominates neighboring slower rhythm, surviving as a “winner” by macroscopic lateral inhibition. Thus, the random-to-organized patterning of OPWs proceeds by self-organization within the caecum, in which two distinct mechanisms, at least, are employed; suppressive actions by primitive waves followed by macroscopic lateral inhibition.

KEYWORDS

chicken embryo, gut development, peristaltic wave, optogenetics, self-organization

Introduction

Gut peristalsis is a series of wave-like movements of a local contraction along the gut axis. Peristaltic movements propel internal contents, and are essential for nutrient digestion and absorption. Dysregulation of peristalsis is associated with many intestinal disorders underscoring the importance of understanding the mechanisms underlying the peristaltic movements. Peristaltic movements have extensively been studied for adult guts, in which distinguishment between extrinsic effects (e.g., mechanical stimulation by ingested material) and intrinsic mechanisms has been a challenge. To circumvent these, the embryonic gut has emerged to serve as a powerful model since it undergoes peristaltic movements without ingested contents (Chevalier et al., 2017; Shikaya et al., 2022).

The gut of chicken embryos is particularly useful since the spatial information along the entire gut can be obtained due to spatial landmarks along the gut axis. We previously reported a distribution map of origins of peristaltic waves (OPWs), which are sites

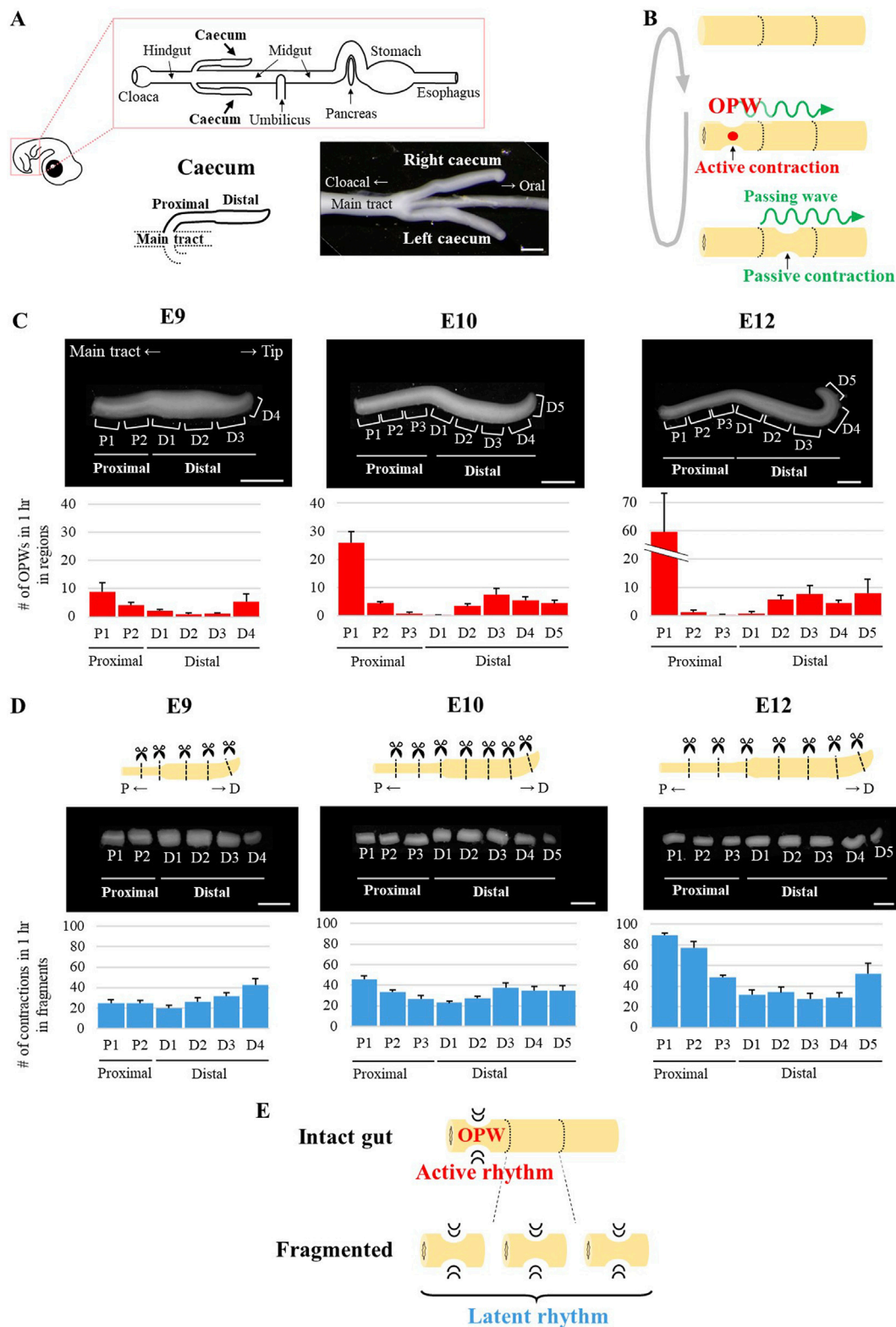


FIGURE 1

Spatial patterning of OPWs and latent rhythms during chicken caecum development. **(A)** Schematic representation of the chicken embryonic digestive tract (upper panel). Magnified view of the E10 caeca, shown as symmetrical protrusions from the main tract (lower panels). Scale bar, 1 mm. **(B)** Two types of gut contractions: 1) Active contraction: a spontaneous contraction at the site of OPW generation (red circle); 2) Passive contraction: a contraction induced by a passing wave (green wavy lines). **(C, D)** Developmental changes in the number of OPW generations in 1 h in each region **(C)** and the number of contractions in 1 h in each fragment **(D)** of the caecum. P, proximal; D, distal. Bar graphs and error bars represent average and standard error, respectively (n = 5 for each embryonic stage). Scale bars, 1 mm. **(E)** Summary diagram of Figure 1. In an intact gut, a specific region exhibits an active rhythm characterized by OPW generation. Upon separation, each fragment initiates its own distinct latent rhythm.

undergoing spontaneous contraction followed by wave propagation, in the entire gut posterior to the duodenum. The map demonstrated that OPWs are progressively confined to specific sites along the gut axis as development proceeds (Shikaya et al., 2022).

In the present study, we asked how OPWs are confined to specific sites using an embryonic caecum as a model. Unlike mammals, most avians possess a pair of caeca that protrude in a lateral-to-anterior direction from the main tract at the border between midgut (ileum) and hindgut (Figure 1A). In chickens, left and right caeca elongate in parallel as straight tubular structures. These characteristics offer advantages; one part of caeca is used for experimental manipulation with the other being for control, minimizing complexities of variations between embryos. In addition, a short and straight shape facilitates quantitative assessment of OPW locations along the tubular structure, which is a challenge with a long and convoluted midgut. We demonstrate that while prominent OPWs are seen in the terminal endpoints of the caecum, whereas the middle region of the caecum displays less. However, when the caecum is fragmented into several small pieces along the gut axis, every piece commences to exhibit an OPW activity (spontaneous contraction) with their own contraction rhythm, unveiling latent rhythm possessed by every region along the caecum. Short-term (4 h) monitoring shows that among subtle differences in latent rhythm along the caecum axis, a region with faster clock survives as a “winner” (OPW) by suppressing its neighbors’ rhythm of slower clock. In addition, a long-term study (3-day culture) reveals that the more frequently a given region experiences passing waves coming from OPWs, the slower rhythm this region acquires. Our findings provide evidence that patterning/positioning of OPWs along the gut is specified, at least in part, by two distinct types of self-organization mechanisms within the gut, long-term suppressive actions by passing waves followed by short-term macroscopic lateral inhibition.

Materials and methods

Chicken embryos

Fertilized chicken eggs were obtained from the Yamagishi poultry farms (Wakayama, Japan), and embryos were staged according to Hamburger and Hamilton (HH) series (Hamburger and Hamilton, 1992) or embryonic day (E). All animal experiments were conducted with the ethical approval of Kyoto University (#202408).

Short-term *ex-vivo* culture

Most experiments for short-term observation of gut motility (approximately less than 5 h) were performed using the following culture conditions: Caeca were dissected from E9, E10, and E12 embryos and placed in a silicone-coated Petri dish (6 cm diameter) containing 13–15 mL of high-glucose DMEM (Wako, 048–29785) supplemented with 1× Penicillin-Streptomycin-Amphotericin B Suspension (PSA) (FUJIFILM, 161–23181). The Petri dish was maintained in a heating chamber (BLAST, C-140T and BE-051A) at 36.0°C under an atmosphere of 5% CO₂ and 95%

air. Six (proximal-1 to 2 and distal-1–4) and eight (proximal-1 to 3 and distal-1–5) equal-sized regions were defined in E9 caecum and E10, 12 caeca, respectively (Figure 1C). Intact caeca (separated from the main tract) were imaged under free-moving conditions to minimize mechanical stress (Figures 1C, 3A). In contrast, fragmented caeca based on each region (Figures 1D, 3B lower; Figure 4D right; Figure 4E right) were imaged within PDMS canals (internal dimensions: 0.8 mm × 1 mm) to prevent drift. Caeca were cultured for 2–4 h until irregular gut movements subsided. Time-lapse images were acquired every 1-s for 1 h using a Leica MZ10 F microscope equipped with a DS-Ri1 camera (Nikon). Image analysis of each region/fragment was performed using NIS Elements ER (Nikon, version 5.21.00). Images were processed and converted to intensity values, and the number of contractions was manually counted with the aid of image analysis.

Provocation of the gut fragment contraction

The proximal 2 regions (P2) of E12 caeca were prepared as described above (Short-term *ex-vivo* culture). Caecal fragment was placed in a 3D-printed holder (made by Prusa i3 MK3S+) and fixed in a culture dish. To induce artificial gut contractions, a homemade mechanical stimulator was employed. A tungsten wire (Nilaco, 461167, 0.10 mm diameter) attached to a glass capillary was connected to a piezo bending actuator (THORLABS, PB4NB2W) via 3D-printed adaptors. The piezo actuator was controlled by a function waveform generator (Siglent, SDG1032X) via piezo driver (MESS-TEK, M-2691) with the following settings: Period, 1000 s; Amplitude, 3.000 Vpp; Offset, 0.000 Vdc; Pulse Width, 200.000 ms; Rise Edge, 16.8 ns; and Delay, 10 ms. This configuration ensured that the tungsten wire tapped the gut fragment immediately upon the movement of the actuator. The position of piezo bender was carefully adjusted with micromanipulator (Narishige, M-152) to tap appropriate region and avoid damaging the caecum fragment.

Long-term *ex-vivo* culture

For 3-day incubation experiments (Figure 3B upper panel; Figures 4C, D left panel; Figure 4E left panel), caeca were dissected from E10 chicken embryos and placed in PDMS canals (internal dimensions: 0.7 mm × 1 mm) attached to a 6 cm diameter Petri dish containing 15 mL of high-glucose DMEM (Wako, 048–29785). The Petri dish was maintained in a heating chamber (BLAST, C-140T and BE-051A) at 38.5°C under 95% O₂ and 5% CO₂. Oxygen was supplied by an oxygen generator (KMC, M1O2S10L). For experiments shown in Figure 3B upper panels, one caecum was randomly selected, and its proximal-1 (P1) and –2 (P2) regions were removed. The other caecum was left intact. For experiments shown in Figure 4D left and 4E left panels, the P1 and P2 regions were removed from both caeca. Data from paired caeca were analyzed as control and intervention conditions. Time-lapse images were acquired every 1-s for 3 days, and contractions of distal-2 (D2) region were converted to intensity values using NIS Elements ER. A custom Python script (see Data analysis) was used to automatically detect passing waves as intensity peaks. In cases

where automatic detection was unreliable, the number of contractions was manually counted.

In ovo electroporation

In ovo electroporation was performed as previously described (Momose et al., 1999; Atsuta et al., 2013) with slight modifications. Briefly, a DNA solution was prepared at a concentration of 10 µg/µL, containing pT2A-CAGGS-ChR2(D156C)-mCherry-IRES-Neor: pCAGGS-T2TP: 4% fast green FCF (Wako, CI 42053) at a ratio of 4:1:0.5. This solution was injected into the coelomic cavity of the lateral plate mesoderm on the right side of Hensen's node (presumptive right caecum) of E2.5 (HH13-15) stage embryos (Shikaya et al., 2023). An electrical pulse of 50 V, 0.05 ms duration was applied, followed by five pulses of 7 V, 25 ms duration, at 250 ms intervals (BEX, Pulse generator CUY21EDITII). Electroporated embryos were incubated *in ovo* at 38.5°C with high humidity until E10 stage. Fluorescent images were acquired using a Leica MZ10 F microscope equipped with a DS-Ri1 camera (Nikon)

Optogenetics

A pair of caeca, the right one expressing ChR2(D156C)-mCherry, was obtained from the E10 electroporated embryo described above. Right caecum expressing ChR2(D156C) served as the experimental group, while left caecum served as an internal control. Both caeca were dissected from the main tract, and the proximal-1 (P1) and -2 (P2) regions were removed. The caeca were then incubated using the previously described "Long-term *ex-vivo* culture" method. Blue light ($\lambda = 470$ nm) was generated by an LED (OSB56L5111P) and delivered focally to the distal-3 (D3) and -4 (D4) regions of the right (electroporated) caecum via a 500 µm diameter optical fiber. The fiber was inserted through a small hole in the lid of the Petri dish and positioned close to, but not in contact with, the specimen. Light pulse irradiation (40 ms pulse width, every 30 s) was controlled by a microcomputer Arduino Uno (arduino.cc). Irradiation typically induced the generation of OPWs at the irradiated region. These OPWs then propagated to the distal-2 (D2) region, observed as passing waves. Time-lapse images were acquired under red light ($\lambda = 590$ nm, Opto Code, EX-590 and LED-EXTA) for 3 days to minimize unintended activation of contractions. The number of passing waves in the D2 region was visually counted with the aid of NIS Elements ER analysis software. The number of contractions (times/hour) was calculated for the passing waves observed during organ culture. After 3 days of incubation, the D2 region was isolated from the specimens under red-light conditions. Time-lapse recordings were then performed to assess the number of contractions (in 1 h) in the isolated region under "Short-term *ex vivo* Culture" conditions.

Data analysis

Statistical analysis and graph construction were performed using Microsoft Excel. Paired t-tests were used to statistically compare the

data presented in Figures 3, 4. Statistical significance was defined as * $P < 0.05$ and NS indicating not significant. Bar graphs and error bars represent the means and standard errors, respectively. Peaks associated with gut contractions were automatically detected using a SciPy library (scipy.signal.detrend, standardize, and find peaks) in Python. In cases where the automated detection was insufficient, peaks were manually counted.

Results

Spatial patterning of OPWs during caecum development

In this study, we define terms as follows: a spontaneous contraction at the site of OPW is called active contraction, and a contraction on the way of passing (propagating) wave is a passive contraction (Figure 1B). Elongating caeca at E9 to E12 display a landmark at the middle along the proximal-to-distal (PD) axis; the proximal and distal portions are thinner (small in diameter) and thicker (large in diameter), respectively (Figure 1A).

Caeca from E9, E10 and E12 embryos were excised from the main tract, and subjected to video monitoring for OPWs using an *ex vivo* culture method (see Materials and Methods). To precisely locate OPWs along the caecal axis, we divided the proximal and distal portions further into several regions (Figure 1C, Supplementary Movies S1, S2). The number of contractions in 1 h (frequency) in each region is shown in Figure 1C. From E9 to E12 examined, originally indifferent frequency became differentiated between regions. For example, the proximal 1 region (P1) exhibited an increase in frequency during the time of development; 8.9 (E9), 26 (E10), and 59.6 (E12), whereas the frequency decreased in region P2; 4.1 (E9), 4.4 (E10), and 1.2 (E12). Of note, P2, P3 and D1 displayed no or few OPWs, if any, at E12 (Figure 1C). Thus, the difference in OPW frequency among regions became enhanced indicating that OPWs undergo spatial patterning during caecal development.

To exclude the possibility that an amputation would affect the prominence of P1, we examined OPW frequencies in intact caeca connected to the main tract (E12). Overall trend of OPW frequencies along the caecal axis (high in proximal and distal regions, low in middle regions) were highly consistent before (Supplementary Figure S1) and after the separation (Figure 1C, E12). And when we amputated in between P3 and D1, which would normally display low OPWs, the OPW frequency in D1 was unchanged (compare Supplementary Figure S2A and Figure 1C, E12). Thus, the high frequency of OPW generation in P1 region is primarily due to its intrinsic capacity, and not by artifact of amputation.

Latent rhythm was unveiled in non-OPW regions when isolated from neighbors

How are OPWs confined to specific regions in the caecum at E12? Two possibilities are raised; one is that non-OPW regions (P2, P3, D1) have lost their contraction ability by E12. Alternatively, contraction abilities are retained in these regions but somehow

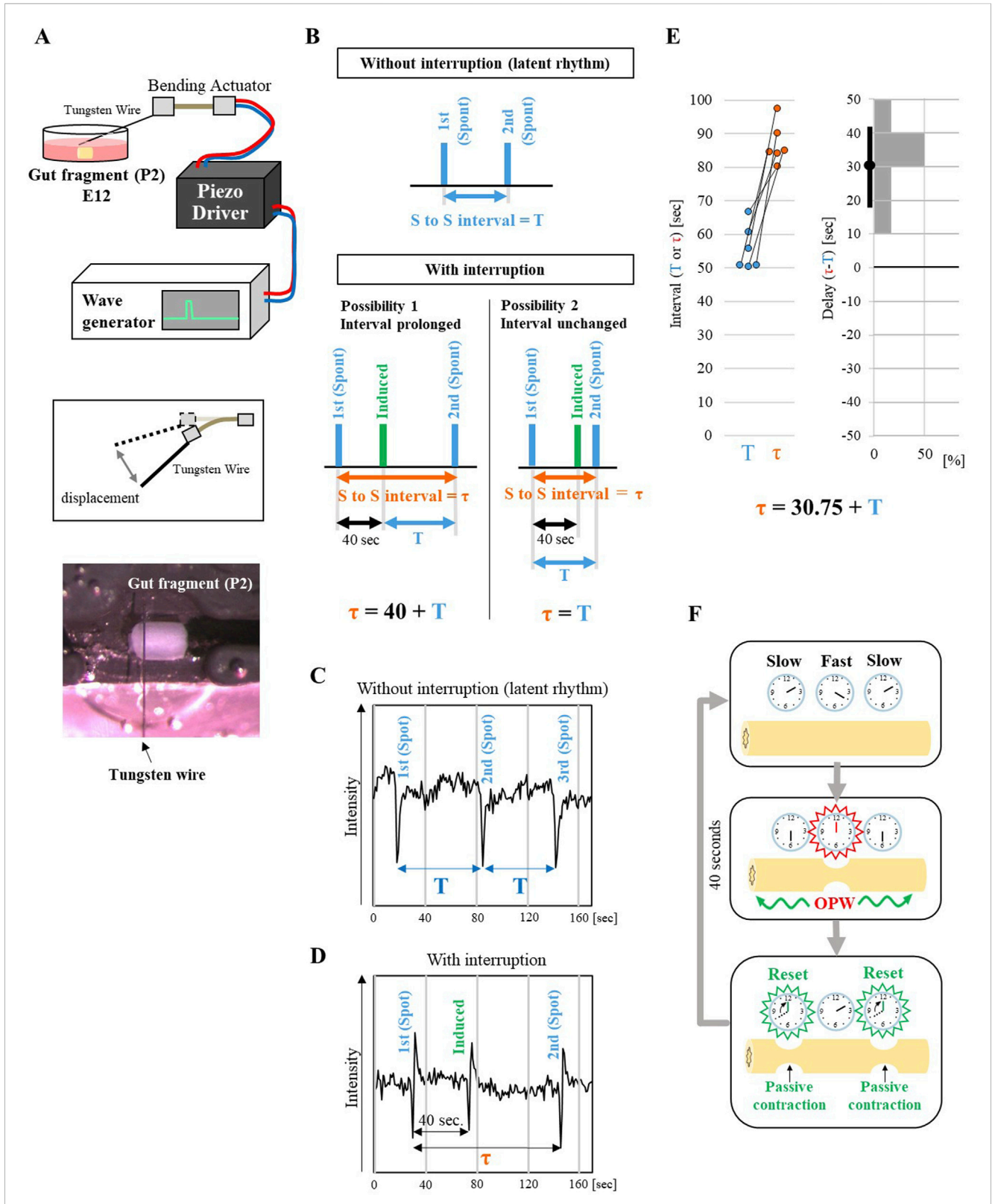


FIGURE 2
Resetting of the latent rhythm by an ectopically induced contraction. (A) Schematic of the mechanical stimulator setup. An E12 gut fragment (P2) in *ex vivo* culture was tapped by a thin tungsten wire attached to piezo bending actuator. The actuator was controlled by a wave generator via a driver (see Materials and Methods). The bottom panel shows an actual image of the tapping setup. (B) Expected results of rhythm interruption. Upper panel indicates the latent rhythm of P2 fragment without interruption. The interval between first and second spontaneous contractions (blue bars) is defined T. Lower panels indicate two possible outcomes with interruption. Upon an induced contraction by tapping (green bars), the interval between the first and second spontaneous contractions after the interruption (τ) can either be prolonged ($\tau = 40\text{ s} + T$) or remain unchanged ($\tau = T$). Representative data of temporal changes in P2 contractions without (C) and with interruption (D). Rapid changes in the traces represent spontaneous or induced contractions. (E) (Continued)

FIGURE 2 (Continued)

Quantification of the effects of interruption. The left graph shows the spontaneous interval without interruption (T) and with interruption (prolonged interval (τ)). Pairs of dots connected with a line represent the same specimen ($n = 6$ embryos). The right histogram shows the delay (difference between τ and T) in the latent rhythm caused by the interruption. The average of the delay and 95% confidence interval are shown as black dot and bar, respectively. (F) A model for rhythm resetting. Clocks represent the frequencies of latent rhythms. A faster clock in the middle generates OPWs that propagate to neighboring slower clocks and reset their rhythms. This mechanism allows the faster clock (higher latent rhythm) to maintain its rhythm and suppress the emergence of OPWs in slower clocks (slower latent rhythm).

suppressed. To distinguish between these two, the E12 caecum was chopped into pieces to obtain fragments of P1 to D5, and assessed for contractions in each piece. Markedly, non-OPW fragments (P2, P3, D1) exhibited active contractions (Supplementary Movie S3, Figure 1D). The frequency in fragment P1, which already showed the highest in unfragmented (intact) caecum (Figure 1C), was higher than fragment P2, and the same holds true for D5 (higher) and D4 (lower) in E12. In addition, when P1 was removed from an intact caecum at E12, P2 exhibited a markedly enhanced rhythm (1.8–35.6) (Supplementary Figure S2B). Following dissection of E9 caeca into six fragments (P1–P2; D1–D4) and E10 caeca into eight fragments (P1–P3; D1–D5), we observed that the distribution of frequencies across these regions, particularly the proximal regions, was less diverse in E9 embryos than in E10 embryos. It is highly conceivable that the basal line of this distribution increased and became progressively differentiated during development as shown in Figure 1D.

These findings suggest that: 1) every region in the cecum possesses the ability to generate active (spontaneous) contractions, hereafter called “latent rhythm”, 2) the latent rhythm in non-OPW regions (P2, P3, D1) is suppressed by neighboring high- OPW regions, and 3) Such differences in latent rhythms between juxtaposed regions are gradually formed during development.

The latent rhythm is reset by interrupted contraction

Given that fragments P2–D1, which are normally non-OPW-generating regions in the intact caecum, exhibit latent rhythm upon isolation, we hypothesized that passing waves coming from a neighboring high rhythm OPW (e.g., P1) might mask the latent rhythm in intact caecum. To understand how this masking is regulated, we examined a reaction of a non-OPW-generating fragment (for example P2) to an ectopically induced contraction (interruption) that mimics a passive contraction forced to occur by a passing wave. Since a normal interval between spontaneous contractions (latent rhythm) of P2 at E12 was around 50 s (estimated from Figure 1D), we gave a mechano-stimulation by tapping at 40 s after a first spontaneous contraction. A tapping with a tungsten wire controlled by a piezo actuator evoked contractions in fragment P2 in a consistent manner (Figure 2A, Supplementary Movie S4). This direct tapping of P2 is the most available/feasible way allowing for precise control over the timing and location of the stimulus since evaluating an impact on P2 by provoking passing waves from a distant site is currently unavailable.

Two possibilities for the P2 reaction were conceived. 1) The interval of latent rhythm would be delayed by the interruption; $\tau = 40 + T$ (T = normal interval of latent rhythm without interruption

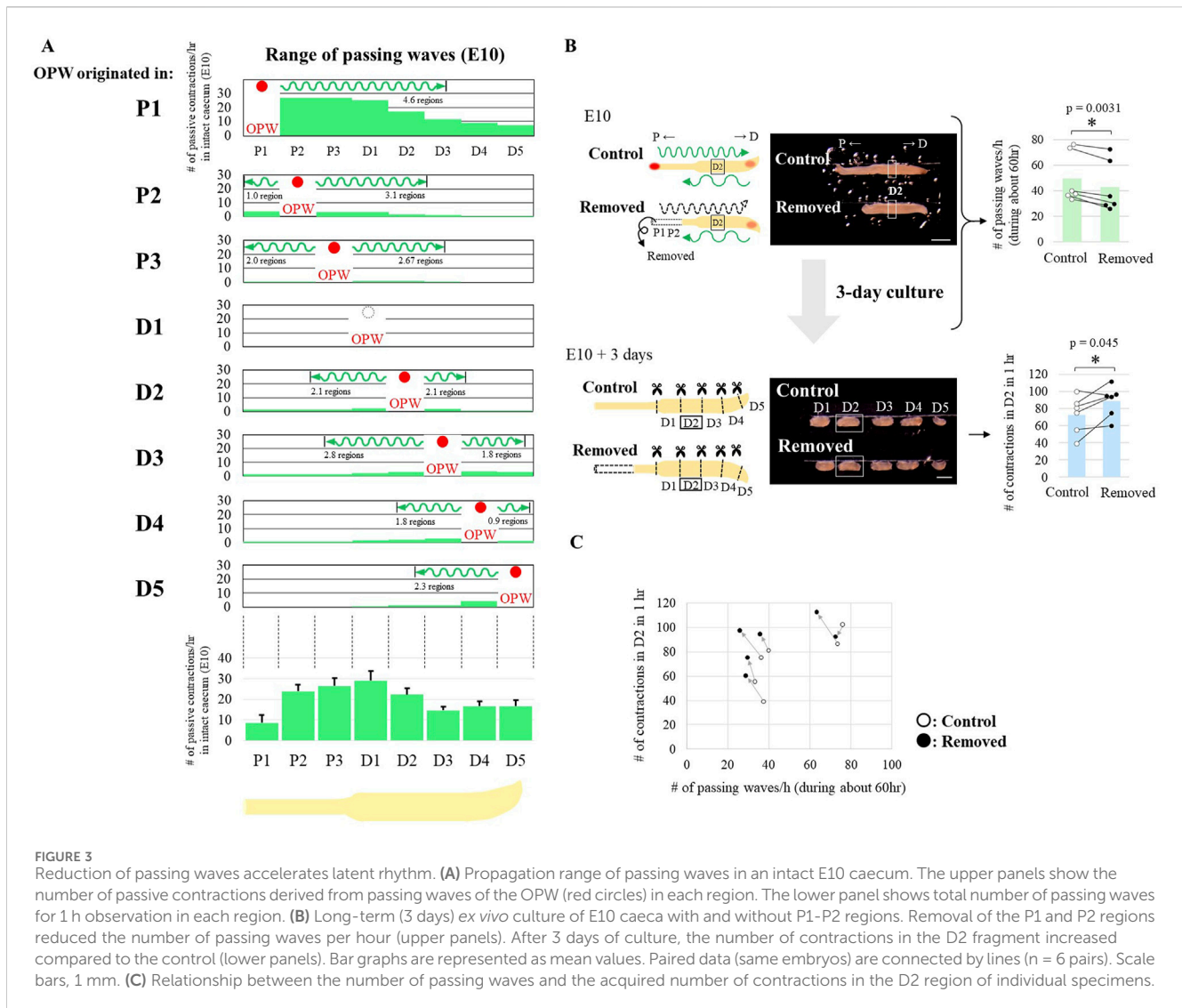
shown in blue arrow, Figure 2B, τ = total time (orange arrow) between the first and second spontaneous contractions (blue bars with interruption). 2) The latent rhythm would not be affected by the interruption; $\tau = T$ (Figure 2B). Monitoring analyses showed that with a tapping interruption, the second spontaneous contraction took place at 86.83 s after the first one (Figures 2C, D, Supplementary Movie S4; Figure 2E for paired comparison). Thus, $\tau = T + 30.75 \pm 4.40$ (average \pm standard error), a result that is closer to the first possibility, that the interval of latent activity is delayed by the interruption.

With these findings, we propose a model as shown in Figure 2F. Originally, every region in the embryonic caecum possesses its own “clock” of periodic contractions, which is slightly diverse between each other along the caecum axis. Among them, a region with faster clock emits propagating waves that force “passive” contractions in neighboring regions that have slower clock. Subsequently, the forced contracted regions “reset” their clock to count from zero. In this way, waves coming from a faster(est) clock defined as an OPW(s) continuously force passive contractions in neighboring slow regions, whose latent rhythm remains masked. We call these suppressive processes as “macroscopic lateral inhibition” in the gut, which is likely mediated by oscillatory entrainment known in physiology and neurobiology (Diamant et al., 1970; Van der Pol, 1929; Perkel et al., 1964).

Latent rhythm was augmented with a reduced number of passing waves

Given that the spatial differences in latent rhythm (Figure 1D) are the basis for self-organized sharp patterning (Figure 1C) through macroscopic lateral inhibition (Figure 2), we further explored how the differences in latent rhythm are generated at earlier stages of gut development. Because a non-OPW region is forced to contract (passive contraction) by an OPW-derived wave that passes over this region (passing waves), and also because such forced contractions reset the clock (Figure 2), we reasoned that the differences in frequency of passing waves that are experienced by each region plays a role in shaping the differential patterns of latent rhythm along the caecum.

To address this, we examined a range of passing waves emitted from different sites of OPWs at E10. For example, as already shown in Figure 1C, many waves were emitted from P1, and a substantial number of these waves vanished near D3 with a few propagating to the end of the caecum (Supplementary Movie S1 and Figure 3A; over 4.6 regions in average). Similarly, waves originated from other regions, although their frequencies were low, also ceased after propagating over 2 or 3 regions (Figure 3A). Thus, the number of passing waves that each region experiences varied between regions; the middle regions experienced more waves, while the number of waves decreased toward both ends of the caecum.



These differential patterns of passing wave experiences along the caecum are complementary with those shown for the latent rhythm (compare the graph in Figure 3A with Figure 1D).

To further comprehend how the passing wave experiences impact the production of latent rhythm, we attempted to reduce the frequency (number) of passing waves. When [P1-P2] was removed from a caecum, [P1-P2]-originated high frequent waves were extinguished leaving less frequent waves coming from distal tip [D4-5] unaffected (Figure 3B, assessed for D2). The number of passing waves in [P1-P2]-deprived specimens did not decrease as significantly as hypothesized, owing to a compensatory increase in OPW generation, primarily within P3. The theoretical basis for this OPW generation is the release of macroscopic lateral inhibition originating from P1 and P2. The [P1-P2]-deprived specimens were *ex vivo* cultured for 3 days, and subjected to assessment of latent rhythm in fragments in a way similar to Figure 1D. Contraction frequency of fragmented D2 was augmented compared with control ($n = 6$ pairs, Figure 3B in light blue), which was further corroborated by paired scatter plot shown in Figure 3C. These findings imply that the passing waves negatively regulates the latent rhythm.

Optogenetically augmented frequency of passing waves declined the latent rhythm

To more precisely scrutinize the role of passing waves in the differential distribution of latent rhythm, we experimentally increased the frequency of passing waves in the caecum using optogenetic methods that we recently developed for embryonic guts (Shikaya et al., 2023). A modified type of channelrhodopsin 2, ChR2(D156C), efficiently responds to blue light irradiation to transmit depolarization signal intercellularly. Tol2-ChR2(D156C) tagged with mCherry was electroporated into the splanchnopleural mesoderm at the presumptive caecum region in the right half of embryo at E2 (Figure 4A). ChR2(D156C)-expressing right- and untreated left caeca were dissected from embryos at E10 (Figure 4B), followed by a removal of the proximal region [P1-P2] to obtain a less frequently waving caecum as shown above (Figure 3). In these analyses, we irradiated blue light into D3/D4 at 30 s intervals, which successfully evoked peristaltic waves passing at least over D2 with the rhythm obeying the irradiation cycle (Figure 4C, Supplementary Movie S5). In this way, D2 region was not

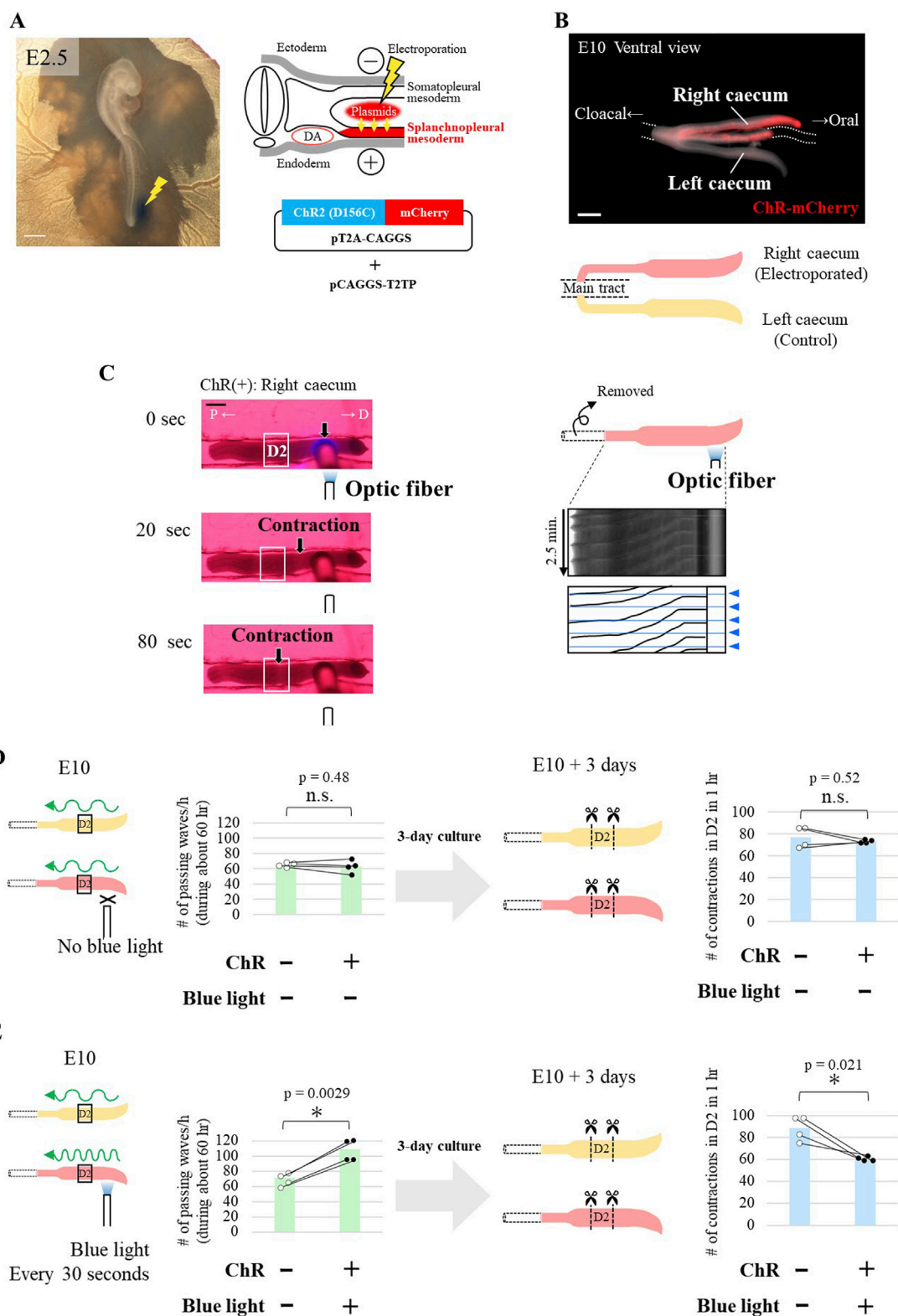


FIGURE 4

Optogenetically-increased passing waves decelerate latent rhythm. (A) *In ovo* electroporation of a Tol2 plasmid encoding channelrhodopsin-2 variant, ChR2(D156C), into the splanchnopleural mesoderm of the right side of the embryo at E2.5 (indicated by yellow zigzag lines). DA, dorsal aorta. Scale bar, 1 mm. (B) E10 caeca expressing ChR2(D156C) in the right caecum and a part of the main tract (dotted lines). The left caecum served as an internal control. Scale bar, 1 mm. (C) Left panels: Time-series images showing artificially induced peristaltic waves in an E10 caecum expressing ChR2(D156C). The P1 and P2 regions were removed. Blue light stimulation of the distal region triggered contractions that propagated to the D2 region (white rectangle). P, proximal; D, distal. Scale bar, 500 μ m. Right panels: Kymographs showing serial peristaltic waves (black slanted lines) induced by 30-s intervals of blue light pulses (blue triangles). (D, E) Long-term *ex-vivo* culture of ChR2-D156C-expressing caeca without (D) and with (E) blue light (Continued)

FIGURE 4 (Continued)

stimulation. The P1 and P2 regions were removed. Green bars represent the frequency of passing waves through the D2 region during the 3-day culture. Blue bars represent the latent rhythm of the D2 fragment after 3 days of culture. Data are represented as mean values. Paired data (same embryos) are connected by lines ($n = 4$ pairs).

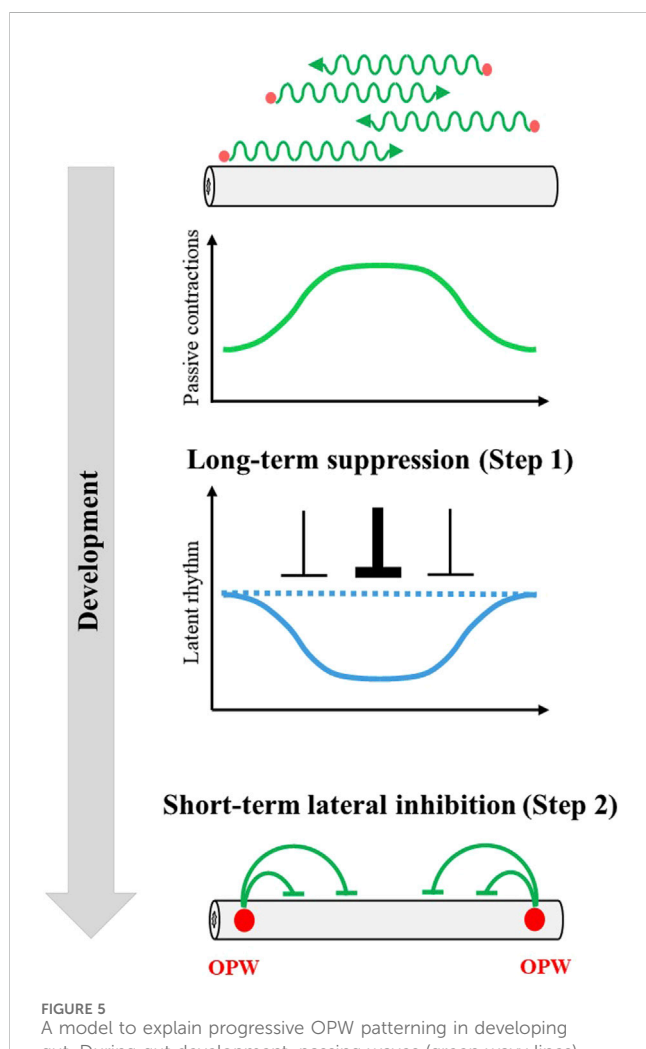


FIGURE 5

A model to explain progressive OPW patterning in developing gut. During gut development, passing waves (green wavy lines) emerge spontaneously at unspecified sites (red circles) along the gut axis. However, fluctuations of emergence of passing waves forms spatial gradient of passing wave frequency (bell-shaped green line) (Figure 3A). This spatial gradient of passing wave frequency shapes a complementary spatial gradient of latent rhythms through long-term suppression (Figures 3B,C, 4). The spatial gradient of latent rhythms ultimately specifies the location of the OPW region through a macroscopic lateral inhibition mechanism (green lines) (Figure 2).

directly irradiated with the blue light. Blue light irradiation by our method did not give detectable effects to the gut peristalsis (Shikaya et al., 2023).

In ChR2(D156C)-expressing right caecum *without* blue light irradiation, contractions in D2 in both intact caecum and fragment were comparable to those in non-electroporated control (left caecum), showing no detectable effects by ChR2(D156C) overexpression (Figure 4D). In contrast, when blue light was irradiated into D3/D4 every 30 s for 3 days, the number of

passing waves were accordingly augmented. Importantly, the latent rhythm in fragment D2 prepared from the irradiated 3-day cultured caecum was significantly reduced (Figure 4E). Thus, the more frequently a given region experiences passing waves, the slower rhythm it acquires (Supplementary Figure S2).

Discussion

We have demonstrated that even non-OPW regions in the embryonic caecum retain an ability to implement active contraction unveiled by fragmentation of the gut. This ability is called latent rhythm in this study, which is normally suppressed in the intact gut. The latent rhythm becomes progressively patterned along the gut, and this patterning serves as the basis for the final confinement of OPWs at later stages. The patterning of OPWs proceeds by self-organization within the gut, where at least two distinct mechanisms are employed (Figure 5). Step 1 is that initially less diverse latent rhythm among regions becomes more diverse/differentiated by the effects of randomly occurring passing waves; the more passing waves a given region experiences to undergo forced/passive contractions, the less frequent rhythm this region acquires. Step 2 is that a region with faster clock of latent rhythm that is generated by Step 1 dominates neighboring slow clock to survive as a winner. Step 2 is regarded as a process of macroscopic lateral inhibition mediated by entrainment. Both Step 1 and Step 2 employ suppressive actions of long-term (3 days) and short term (< 1 minute), respectively.

Roles of precocious waves in the patterning of latent rhythm

While it is well known that peristaltic movements are important for the transportation of internal contents in adults, other roles of these movements remained poorly explored. In the current study using embryonic gut, we demonstrate that frequencies of peristaltic passing waves regulate negatively the latent rhythm. In [P1-P2]-lacking caecum showing a reduced number of passing waves, the latent rhythm was augmented after 3 days (Figure 3). Conversely, when more passing waves were experimentally provided, the latent rhythm was declined. In early embryonic guts including caecum, primitive peristalsis-like movements occur randomly, where many waves vanish before reaching to the end (Chevalier et al., 2017; Shikaya et al., 2022 and this study), but the roles of these primitive/precocious waves have not been well understood. Our findings suggest that these waves in early guts negatively regulate the latent rhythm; the more frequently a given region experiences passing waves to undergo forced contractions, the slower latent rhythm it acquires. These negative regulations generate differential distribution of latent rhythm along the gut axis, which later shapes spatial patterns of OPWs by macroscopic lateral inhibition (see also

below). The evidence to explain the regulation of OPW positioning by precocious peristaltic waves is unprecedented. How passing waves negatively impact on latent rhythm has yet to be studied. It was previously reported that reiterative stimulations by stretching cardiomyocyte *in vitro* resulted in converting its rhythm (Nitsan et al., 2016), although this case was a positive correlation contrasting with our findings with a gut specimen.

Macroscopic lateral inhibition of latent rhythm shapes the OPW positioning in embryonic gut

We have also found that in developing guts the differentiated patterns of latent rhythm generated by precocious passing waves (Step 1) is further subjected to macroscopic lateral inhibition, in which a region with faster-counting rhythm dominates its neighbors' slow-counting regions (Step 2). A region having slower latent rhythm needs to obey faster rhythm to undergo forced/passive contraction without an opportunity to exert its own latent rhythm of active contraction. In such actions, also known as entrainment, a slow-counting region resets its rhythm when encountered with a faster rhythm (Figure 2). If freed from entrainment, the latent rhythm can quickly be retrieved (as seen for augmented contractions in P2 in P1-lacking caecum, Supplementary Figure S1). The macroscopic lateral inhibition described in the current study is conceptually reminiscent of widely known lateral inhibition acting at the microscopic level, where Notch/Delta signaling mediates. In both micro- and macroscopic levels, initially equal properties become differentiated by mutual suppressive actions. Considering organs that are very long such as gut, long-range signals must be at work to coordinate patterning and growth, and it is sensible that the macroscopic lateral inhibition demonstrated in this study is one of the mechanisms that explain such organ-level coordination.

Latent rhythm (or its equivalent phenomena) in the gut was previously reported using adult intestine in felines (Diamant and Bortoff, 1969), where they proposed that linearly graded latent rhythm yields distinct sharp boundaries between contraction and non-contraction areas. More recently, a study using felines showed that when a region with fast rhythm in the intestine was occluded, a neighboring region started to exert a contraction rhythm, although slower than the occluded area (Lammers and Stephen, 2008). Thus, the macroscopic lateral inhibition that we described in the current study could be a general mechanism underlying the patterning of peristaltic movements in the gut. Unlike studies with adult guts, our study addressed a transition from initially random patterns of early peristaltic movements to confined positioning at later stages, where macroscopic lateral inhibition (Step 2) is based on precocious conditions of passing waves (Step 1).

Regarding the entrainment in biological rhythm, similar phenomena have been described in cardiac pacemaker physiology. When the primary pacemaker of sinoatrial (SA) node becomes defective, latent rhythm of atrioventricular (AV) node, the second pacemaker, is retrieved and compensates for the failure of SA, although its rhythm is slower than that of SA (Zahn, 1913; Grant, 1956; Waldo et al., 1984; Schamroth et al., 1988). These notions suggest a similarity between heart and gut, and might help

unveiling the molecular and cellular mechanisms underlying OPW-positioning in the gut.

Data availability statement

The raw data supporting the conclusions of this article will be made available by the authors, without undue reservation.

Ethics statement

The animal study was approved by Animal Experiment Committee of Kyoto University (#202408). The study was conducted in accordance with the local legislation and institutional requirements.

Author contributions

KK: Conceptualization, Writing–original draft, Data curation, Formal Analysis, Investigation, Methodology. SK: Methodology, Writing–review and editing. SU: Data curation, Methodology, Software, Writing–review and editing. YT: Conceptualization, Funding acquisition, Project administration, Supervision, Visualization, Writing–original draft, Writing–review and editing. MI: Conceptualization, Data curation, Formal Analysis, Funding acquisition, Investigation, Methodology, Project administration, Resources, Software, Supervision, Validation, Writing–original draft, Writing–review and editing.

Funding

The author(s) declare that financial support was received for the research, authorship, and/or publication of this article. This work was supported by JSPS KAKENHI Grant Numbers: 21K06198 (MI), 23H04702 (MI), 23H04933 (YT) and 23K19369 (SK); and by FY 2022 Kusunoki 125 of Kyoto University 125th Anniversary Fund (MI).

Acknowledgments

We thank Prof. Scott Gilbert for careful reading of the manuscript and discussion. We also thank Prof. Shinya Kawaguchi and Dr. Takuma Inoshita for technical advice for the oxygen generator, and National BioResource Project (Chicken-Quail, Nagoya University) for their technical help.

Conflict of interest

The authors declare that the research was conducted in the absence of any commercial or financial relationships that could be construed as a potential conflict of interest.

The author(s) declared that they were an editorial board member of Frontiers, at the time of submission. This had no impact on the peer review process and the final decision.

Generative AI statement

The author(s) declare that no Generative AI was used in the creation of this manuscript.

Publisher's note

All claims expressed in this article are solely those of the authors and do not necessarily represent those of their affiliated organizations, or

those of the publisher, the editors and the reviewers. Any product that may be evaluated in this article, or claim that may be made by its manufacturer, is not guaranteed or endorsed by the publisher.

Supplementary material

The Supplementary Material for this article can be found online at: <https://www.frontiersin.org/articles/10.3389/fcell.2025.1529975/full#supplementary-material>

References

- Atsuta, Y., Tadokoro, R., Saito, D., and Takahashi, Y. (2013). Transgenesis of the Wolffian duct visualizes dynamic behavior of cells undergoing tubulogenesis *in vivo*. *Dev. Growth & Differ.* 55 (4), 579–590. doi:10.1111/dgd.12047
- Chevalier, N. R., Fleury, V., Dufour, S., Proux-Gillardeaux, V., and Asnacios, A. (2017). Emergence and development of gut motility in the chicken embryo. *PLOS ONE* 12 (2), e0172511. doi:10.1371/journal.pone.0172511
- Diamant, N., and Bortoff, A. (1969). Nature of the intestinal slow-wave frequency gradient. *Am. J. Physiology-Legacy Content* 216 (2), 301–307. doi:10.1152/ajplegacy.1969.216.2.301
- Diamant, N., Rose, P., and Davison, E. (1970). Computer simulation of intestinal slow-wave frequency gradient. *Am. J. Physiology-Legacy Content* 219 (6), 1684–1690. doi:10.1152/ajplegacy.1970.219.6.1684
- Grant, R. P. (1956). The mechanism of A-V arrhythmias: with an electronic analogue of the human A-V node. *Am. J. Med.* 20 (3), 334–344. doi:10.1016/0002-9343(56)90118-8
- Hamburger, V., and Hamilton, H. L. (1992). A series of normal stages in the development of the chick embryo. *Dev. Dyn.* 195 (4), 231–272. doi:10.1002/aja.1001950404
- Lammers, W. J., and Stephen, B. (2008). Origin and propagation of individual slow waves along the intact feline small intestine. *Exp. Physiol.* 93 (3), 334–346. doi:10.1113/expphysiol.2007.039180
- Momose, T., Tonegawa, A., Takeuchi, J., Ogawa, H., Umesono, K., and Yasuda, K. (1999). Efficient targeting of gene expression in chick embryos by microelectroporation. *Dev. Growth & Differ.* 41 (3), 335–344. doi:10.1046/j.1440-169x.1999.413437.x
- Nitsan, I., Drori, S., Lewis, Y. E., Cohen, S., and Tzvil, S. (2016). Mechanical communication in cardiac cell synchronized beating. *Nat. Phys.* 12 (5), 472–477. doi:10.1038/nphys3619
- Perkel, D. H., Schulman, J. H., Bullock, T. H., Moore, G. P., and Segundo, J. P. (1964). Pacemaker neurons: Effects of regularly spaced synaptic input. *Science* 145 (3627), 61–63. doi:10.1126/science.145.3627.61
- Schamroth, L., Martin, D. H., and Pachtter, M. (1988). The extrasystolic mechanism as the entrainment of an oscillator. *Am. Heart J.* 115 (6), 1363–1368. doi:10.1016/0002-8703(88)90059-2
- Shikaya, Y., Inaba, M., Tadokoro, R., Utsunomiya, S., and Takahashi, Y. (2023). Optogenetic control of gut movements reveals peristaltic wave-mediated induction of cloacal contractions and reactivation of impaired gut motility. *Front. Physiology* 14, 1175951. doi:10.3389/fphys.2023.1175951
- Shikaya, Y., Takase, Y., Tadokoro, R., Nakamura, R., Inaba, M., and Takahashi, Y. (2022). Distribution map of peristaltic waves in the chicken embryonic gut reveals importance of enteric nervous system and inter-region cross talks along the Gut Axis. *Front. Cell Dev. Biol.* 10, 827079. doi:10.3389/fcell.2022.827079
- van der Pol, B. (1929). Cxxx.a simple proof and an extension of Heaviside's operational calculus for Invariable Systems. *Lond. Edinb. Dublin Philosophical Mag. J. Sci.* 7 (47), 1153–1162. doi:10.1080/14786440608564844
- Waldo, A. L., Henthorn, R. W., Plumb, V. J., and MacLean, W. A. H. (1984). Demonstration of the mechanism of transient entrainment and interruption of ventricular tachycardia with rapid atrial pacing. *J. Am. Coll. Cardiol.* 3 (2), 422–430. doi:10.1016/s0735-1097(84)80030-3
- Zahn, A. (1913). Experimentelle Untersuchungen über Reizbildung und Reizleitung im Atrioventrikularknoten. *Pflüger, Arch. Für Die Gesamte Physiol. Des. Menschen Und Der Thiere* 151–151 (4–6), 247–278. doi:10.1007/bf01705202